



OPEN ACCESS

EDITED BY

Marina Massaro,
University of Palermo, Italy

REVIEWED BY

Francisco Solano,
University of Murcia, Spain
Juan Mancebo-Aracil,
CONICET Institute of Southern
Chemistry (INQUISUR), Argentina

*CORRESPONDENCE

Gianluca M. Farinola,
✉ gianlucamaria.farinola@uniba.it
Fiorenzo G. Omenetto,
✉ fiorenzo.omenetto@tufts.edu

RECEIVED 11 March 2023

ACCEPTED 16 August 2023

PUBLISHED 29 August 2023

CITATION

Lo Presti M, Ostrovsky-Snider N, Rizzo G, Portoghese M, Blasi D, Farinola GM and Omenetto FG (2023), The role of tyrosine in protein-dopamine based bioinspired adhesives: the stoichiometry that maximizes bonding strength. *Front. Front. Biomater. Sci.* 2:1184088. doi: 10.3389/fbiom.2023.1184088

COPYRIGHT

© 2023 Lo Presti, Ostrovsky-Snider, Rizzo, Portoghese, Blasi, Farinola and Omenetto. This is an open-access article distributed under the terms of the [Creative Commons Attribution License \(CC BY\)](https://creativecommons.org/licenses/by/4.0/). The use, distribution or reproduction in other forums is permitted, provided the original author(s) and the copyright owner(s) are credited and that the original publication in this journal is cited, in accordance with accepted academic practice. No use, distribution or reproduction is permitted which does not comply with these terms.

The role of tyrosine in protein-dopamine based bioinspired adhesives: the stoichiometry that maximizes bonding strength

Marco Lo Presti¹, Nicholas Ostrovsky-Snider¹, Giorgio Rizzo², Marina Portoghese², Davide Blasi², Gianluca M. Farinola^{2*} and Fiorenzo G. Omenetto^{1,3,4,5*}

¹SilkLab, Department of Biomedical Engineering, Tufts University, Medford, MA, United States,

²Dipartimento di Chimica, Università degli Studi di Bari, Bari, Italy, ³Laboratory for Living Devices, Tufts University Medford, Medford, MA, United States, ⁴Department of Electrical and Computer Engineering, Tufts University Medford, Medford, MA, United States, ⁵Department of Physics, Tufts University Medford, Medford, MA, United States

Nature has evolved adhesive materials adaptive for several different environments by using versatile chemistry that largely relies on two simple components: catechols and polypeptides. Herein, using dopamine as a catechol compound and several model proteins, we show how the adhesive properties can be tuned by controlling the ratio between catechol units and the tyrosine amino acid residue in the protein components. We found that the best bonding strength performance is obtained using a dopamine molar excess to tyrosine of 8.6 ± 2.9 . Our study points out a general design criterion and process to obtain high-performance adhesives (>2 MPa) starting from cheap, commercially available, and sustainable raw materials.

KEYWORDS

protein-based, dopamine, mussel-inspired, adhesive, sustainable, tyrosine, silk fibroin, catechol

1 Introduction

Various organisms have developed the capability to produce adhesives for purposes such as effective substrate adhesion, prey capture, or armor construction. This has led to the evolution of exceptionally strong and versatile adhesives across different species. Among these, some notable examples are mussels (Priemel et al., 2017), barnacles (So et al., 2017), sandcastle worms (Wang and Stewart, 2013), caddisfly larvae (Bhagat et al., 2016), and tunicates (Zeng et al., 2019). Despite the wide range of organisms and the diverse biological roles of their adhesives, they all share a common chemical moiety, which is the tyrosine-derived molecule 3,4-dihydroxyphenylalanine (DOPA) (Waite, 1990). The oxidation of DOPA permits quinone cross-linking (Waite, 1990) which, in turn, leads to the polymerization of DOPA-containing polypeptides and determines the final adhesion

Abbreviations: BSA, bovine serum albumin; SPH, soy protein hydrolysate; OVA, ovalbumin; WPI, whey protein isolate; DA, dopamine; GPC, gel permeation chromatography; PDA, polydopamine; SF, silk fibroin.

performance. In fact, the entire process is based on DOPA's ability to switch between reduced form (catechol) and oxidized form (quinone) forms responsible for adhesive and cohesive interactions, respectively (Yang et al., 2014; Kord Forooshani and Lee, 2017). The balance between the two forms is dependent on external conditions which includes pH, redox and salinity, and the presence of metal ions that can augment the cross-linking by forming complexes (Degtyar et al., 2014; Silverman and Roberto, 2007; Ahn et al., 2015). Quinone cross-linking has been proposed as the foundation of many bioinspired artificial adhesives, which are generally composed of catechol structures and various guest polymers (Hofman et al., 2018; Sun et al., 2020). Mussel-inspired adhesives remain the most popular (Lee et al., 2011), but there are also examples inspired by barnacles (Yuk et al., 2021), tunicates (Zhan et al., 2017), sandcastle worms (Kaur et al., 2011) and insect cuticle sclerotization (Wang et al., 2020). The quinone cross-linking mechanism and its role in synthetic biomimetic adhesives have been covered extensively in several reviews. (Saiz-Poseu et al., 2019; Krogsgaard et al., 2016; Kord Forooshani and Lee, 2017).

Among adhesive formulations, those based on proteins display distinct mechanical characteristics (Zhou et al., 2018) and provide unique advantages such as biocompatibility, biodegradability, flexibility, high-performance, and sustainability. These properties make such adhesives ideal candidates for the development of biomedical devices (Huang et al., 2018), electronic devices (Lo Presti et al., 2020), sensors (Fratzl and Barth, 2009), and engineered tissues (Place et al., 2009). Furthermore, protein platforms can provide additional levels of molecular organization due to their secondary structures such as α -helices and β -sheets (Webber et al., 2015), which add dynamic mechanical properties to the resulting biomaterials (Lv et al., 2010).

The conversion of tyrosine residues to DOPA is a commonly used technique to mimic the marine organisms adhesion mechanisms and enhance the adhesive characteristics of proteins. Both chemical (Dalsgaard et al., 2011) and enzymatic (Chan Choi et al., 2014) methods are available for this purpose. Nevertheless, these methods require extra synthetic steps and purification procedures, limiting their scalability. Furthermore, the oxidation of tyrosines in proteins leads to side reactions and cross-linking (Burzio and Waite, 2000), reducing their solubility. The use of tyrosinase is often related to the gelation of various proteins (Onwulata and Tomasula, 2010), resulting in decreased adhesive properties. Finally, some studies (Bilotto et al., 2019) have shown that the difference in adhesion based on the oxidation state of tyrosine/DOPA residues is minimal in short peptides with varying levels of these residues. Other factors such as surface chemistry and contact geometry play a more significant role in determining adhesion performance in complex phenomena like adhesion. A simple and convenient approach is represented by the use catechol compounds to modify proteins. Despite the large number of studies on various combinations of catechols and polypeptides for adhesive formulations, the underlying chemical processes which drive the cross-linking have been seldom investigated. This lack of knowledge is likely due to the intrinsic complexity of the structures resulting from quinone cross-linking, whose products are characterized by high molecular weight, insolubility, diverse polymorphism, and by the presence of several functional groups, making structure elucidation very

difficult both for biomimetic and natural materials alike (Waite, 1990). Studies aimed to identify which amino acids in the protein component are involved in the quinone cross-linking reactions have shown cysteine (Kohn et al., 2020; Krüger and Börner, 2021), tyrosine (Bilotto et al., 2019), arginine (White and Wilker, 2011), lysine (Shin et al., 2020) and histidine (Arias et al., 2021) residues to play a significant role both in model and real systems.

Silk fibroin (SF) has been recently proposed as a substrate for quinone cross-linking in the preparation of waterborne biomimetic high-performance underwater adhesives (Presti et al., 2021). SF is a protein with a relatively restricted amino acid composition, predominantly constituted by five amino acids: glycine (Gly) (45% mol), alanine (Ala) (30% mol), serine (Ser) (12% mol), tyrosine (Tyr) (5% mol), valine (Val) (1.8% mol), with the other 15 amino acids making up only 4.7% of residues numerically. Repetitive sequences of the motif Ala-Gly-Ala-Gly-X-Ala, with X = Tyr or Ser, favor the formation of hydrophobic crystalline antiparallel β -sheet domains, which make up about 50% of the native fiber. These crystalline domains are interspersed with hydrophilic disordered regions containing more polar amino acids such as threonine, serine, glutamic and aspartic acid (Rizzo et al., 2020).

Gelatin can be obtained from collagen hydrolysis by acid (type A gelatin) or alkaline (type B gelatin) pre-treatments (Duconseille et al., 2015). Collagen is composed of three α chains forming a triple-helix structure, where the α -chain contains repetitive Gly-X-Y amino acid sequences, X is mostly proline and Y is mostly hydroxyproline. Gelatin, which is predominantly composed of denatured collagens, has a similar amino acid composition to that of collagen molecules, but with partially reformed helices that differ in structure from native collagen.

Caseins are a family of phosphorylated proteins present in the milk transport system which carries poorly soluble nutrients to the offspring. Casein is also able to adsorb on hydrophobic surfaces (Horne, 2002). This behavior is driven by the tyrosine content and block copolymer structure similar to the one of silk fibroin, leading both proteins to a tendency to organize into micelles in solution (Lu et al., 2012).

Soy protein hydrolysate, which is mainly composed of soybean glycinin (Sui et al., 2021), has been investigated for the development of environmentally friendly adhesives due to its high content of hydrophobic amino acids (Mo et al., 2006). Numerous studies have been carried out on the chemical interaction between soy proteins and low molecular weight polyphenols (Ozdamar et al., 2013), revealing binding mechanisms and antioxidant capacity that may be essential in maintaining the reduced state of catechol moieties to preserve adhesion interactions (Kord Forooshani and Lee, 2017).

Serum albumin is the main transporter of fatty acids that are otherwise insoluble in circulating plasma. Bovine Serum Albumin (BSA) is a single-chain protein consisting of 583 amino acids, with a molecular mass of 66.4 KDa and 21 tyrosine residues. The amino acid chain of BSA consists of three distinct domains with a secondary structure composed mainly of α -helical structures (74%), turns, and flexible regions between subdomains. BSA's primary structure is characterized by low levels of tryptophan, methionine, glycine, and isoleucine content, while ionic amino acids such as glutamic acid and lysine are abundant, imparting a high total charge of 185 ions per molecule at neutral pH and

contributing to its solubility (Topalá et al., 2014). Some studies have reported the binding of BSA with small phenolic compounds such as chlorogenic acid (Jia et al., 2023).

Ovalbumin (OVA) is the predominant protein found in egg whites, comprising more than 50% of the total weight of egg white. OVA is a globular protein with a diameter of approximately 3 nm and a molecular weight of around 45 kDa. It consists of 386 amino acid residues, with 50% of these residues being hydrophobic and 30% being acidic side chains (Rostamabadi et al., 2023). Interestingly, OVA has recently gained attention as a potential wood adhesive, highlighting its potential as a bio-based alternative to formaldehyde resins (Lorenz and Frihart, 2023).

Whey, the primary byproduct of the dairy industry, is composed of lactose (71–75 wt%), proteins (10–12 wt%), fats (8–9 wt%), and minerals (4%–10%). With a global production of around 240 million tonnes per year, whey protein isolates (WPI) account for nearly 2 million tonnes. WPI mainly consists of 55% β -lactoglobulin, 25% α -lactalbumin, 10% immunoglobulins, and 10% BSA (Peydayesh et al., 2023).

Herein, using dopamine hydrochloride (DA) as the model catechol compound and *Bombix mori* SF as the model protein, we found that adhesive properties of resulting mixed dopamine/protein glue are dependent by the mass ratio between DA and SF. By conducting the same experiment with proteins other than SF, we observed that the mass ratio of protein to DA varied among different proteins. Therefore, we hypothesized that this variation was dependent on the amino acid composition of the proteins. After performing an amino acid analysis of all the proteins used and comparing the molar concentration of each amino acid to that of dopamine at various concentrations, we found that the molar ratio of DA to tyrosine remained the most consistent compared to all other amino acids under conditions of maximum adhesive performance.

Specifically, we found that the bonding strength performance is maximized when the DA molar excess to tyrosine is 8.6 ± 2.9 (alternatively viewed as an 0.13 ± 0.04 Tyr:DA molar ratio) as measured by lap-shear testing. Hence, we suggest that a DA molar excess of 8.6 ± 2.9 relative to the tyrosine content of a protein optimizes the formation of large pendant oligomers by dopamine, preventing self-polymerization into unbound PDA polymers or the generation of short polydopamine oligomers grafted on isolated protein chains. This hypothesis is supported by gel permeation chromatography (GPC) analysis of the resulting copolymer mixtures.

This study offers a general criterion enabling the production of water-based high-performance adhesive (>2 MPa) by combination of dopamine and inexpensive materials such as proteins from waste products.

2 Materials and methods

2.1 Materials

Bovine Serum Albumin (BSA), Gelatin from porcine skin (type A 175g bloom), Casein from bovine milk, soy protein acid hydrolysate (SPH), Ovalbumin (OVA) bovine thyroglobulin, gallus ovalbumin, equine myoglobin, cytidine, sodium carbonate,

lithium bromide, dopamine hydrochloride and calcium chloride were purchased from Sigma Aldrich and used without any purification. *Bombix mori* cocoons were purchased from Tajima Shoji (Japan) and SF was extracted as described in the following section. Whey protein isolate was purchased from BulkSupplements (Henderson, Nevada).

2.2 Regenerated silk solution preparation

Bombix mori cocoons were degummed by cutting and boiling 10 g of cocoons in 4 L of 0.8 M Na_2CO_3 solution for 30 min to remove sericin, the external glycoprotein coating of the pure fibrous protein. The fibers were washed in deionized water (DI) water then dried overnight at room temperature and immersed in sufficient 9.3 M lithium bromide solution to create a 25% v/w solution and allowed to dissolve for 3 h at 60°C. This silk solution was dialyzed against 4 L of nanopure water using a nitrocellulose dialysis tubing (3.5 kDa MWCO), with water changed 5 times over 3 days to fully remove lithium bromide from the solution. The dialyzed silk solution was then filtered (70 μm , nitrocellulose), centrifuged (11,000 RCF, 20 min, 4°C) then filtered again (0.45 μm , nitrocellulose) to remove debris.

Silk solution concentration was determined by weighing a known amount of solution pre- and post-drying overnight at 60°C. Regenerated silk solution (RSF) was concentrated, if needed, up to 7% (w/v) corresponding to 70 mg/mL by pouring it into a 3.5 kDa MWCO dialysis tubing and placing it into a drying chamber. After dialysis, the solution was stored at 4°C until used.

2.3 Protein-DA solution preparation

All the selected proteins (SF, Casein, SPH, BSA, OVA, WPI and Gelatin) were dissolved in nanopure water to create 7% (w/v) solutions. To improve casein solubilization, 1–5 drops of CaCl_2 (1 M) and NaOH (1 M) were added.

For each protein, 7 different dilutions with different DA-Protein mass ratio (Table 1) were prepared (70.00, 55.22, 41.41, 27.61, 7.00, 3.50, and 0 mg/mL). The solutions were left to polymerize at room temperature for 3 days prior to their deposition for the lap-shear test.

2.4 Adherent preparation and lap-shear test

Appropriate volumes (Table 1) of the protein-DA solution were cast on a single joint of stainless-steel adherent such that a total of 12 mg (dry weight) of the adhesive covered an area of 25×7 mm.

After drying at room temperature, the films on the adherents were activated with 10 μL of either nanopure water or FeCl_3 solution (300 mM) (see SI Supplementary Figure S4). The adherents were then joined together, the joint compressed with a binder clip (25 N) and cured for 2 days at 60°C as previously described (Wang et al., 2020). All specimens broke due to cohesive failure during mechanical testing.

Bonding strength tests were performed on an Instron 3,366 universal testing machine equipped with a 10 kN load cell (Norwood, MA, United States) following a modified version of the ASTM method D1002-10 (38). The testing program applied a shear

TABLE 1 The formulation of the various protein/DA mixtures, their specific DA molar excess to tyrosine ratio according to tyrosine quantification and volumes for casting in constant-mass adhesive lap-shear tensile testing. The DA molar excess to tyrosine that have resulted in higher adhesion performances are in bold.

DA concentration [mg/mL]	Ratio DA/ Protein [g/g]	Casein DA molar excess [mol/mol]	Silk DA molar excess [mol/mol]	SPH DA molar excess [mol/mol]	BSA DA molar excess [mol/mol]	OVA DA molar excess [mol/mol]	WPI DA molar excess [mol/mol]	Gelatin DA molar excess [mol/mol]	Cast volume [μ L]
0	/	/	/	/	/	/	/	/	171
3.5	0.05	0.7664	0.4011	1.1915	0.9653	1.1577	1.9428	5.3360	163
7	0.1	1.5329	0.8022	2.3831	1.9306	2.3155	3.8857	10.6720	156
27.6	0.4	5.3653	2.8079	8.3408	6.7573	8.1045	13.6000	37.3521	123
41.4	0.6	8.4313	4.4125	13.1071	10.6187	12.7357	21.3714	58.6962	108
55.2	0.8	11.1140	5.8165	17.2775	13.9974	16.7880	28.1714	77.3723	96
70	1	13.7967	7.2205	21.4479	17.3761	20.8402	34.9714	96.0483	86

rate of 0.5 mm s^{-1} and continued until failure. The maximum shear load was divided by the bond area (175 mm^2) to calculate bonding strength. Five replicates were measured for each protein/DA mixture.

2.5 GPC

Native and polydopamine-modified proteins were analyzed with an Agilent 1,260 Infinity II HPLC system, separated by an Agilent Aquagel-OH mixed M size exclusion column (PL1149-6801) and detected by UV-Vis absorption with a variable wavelength detector module. The mobile phase was 8.0 M Urea buffered with 10 mM sodium phosphate pH 7.0. Samples were detected at 280 nm which corresponds to absorption by both protein aromatic side chains and polydopamine, and at 330 nm , which corresponds to strong absorption from polydopamine with negligible contribution from proteins (Nam et al., 2018) (Supplementary Figure S5), allowing to distinguish between SF DA-modified and pristine SF.

Molecular weight calibration was performed using protein standards bovine thyroglobulin, bovine serum albumin, *gallus* ovalbumin, equine myoglobin, and cytidine.

2.6 Amino acid analyses

Amino acid analyses of casein, silk fibroin, SPH, BSA, OVA, and gelatin was performed by proteomics & peptide synthesis core at Michigan medical school, MSRB II (Rms C568 & C570C) 1150 W Medical Center Dr, Ann Arbor, MI. Amino acid composition of WPI was provided by the manufacturer.

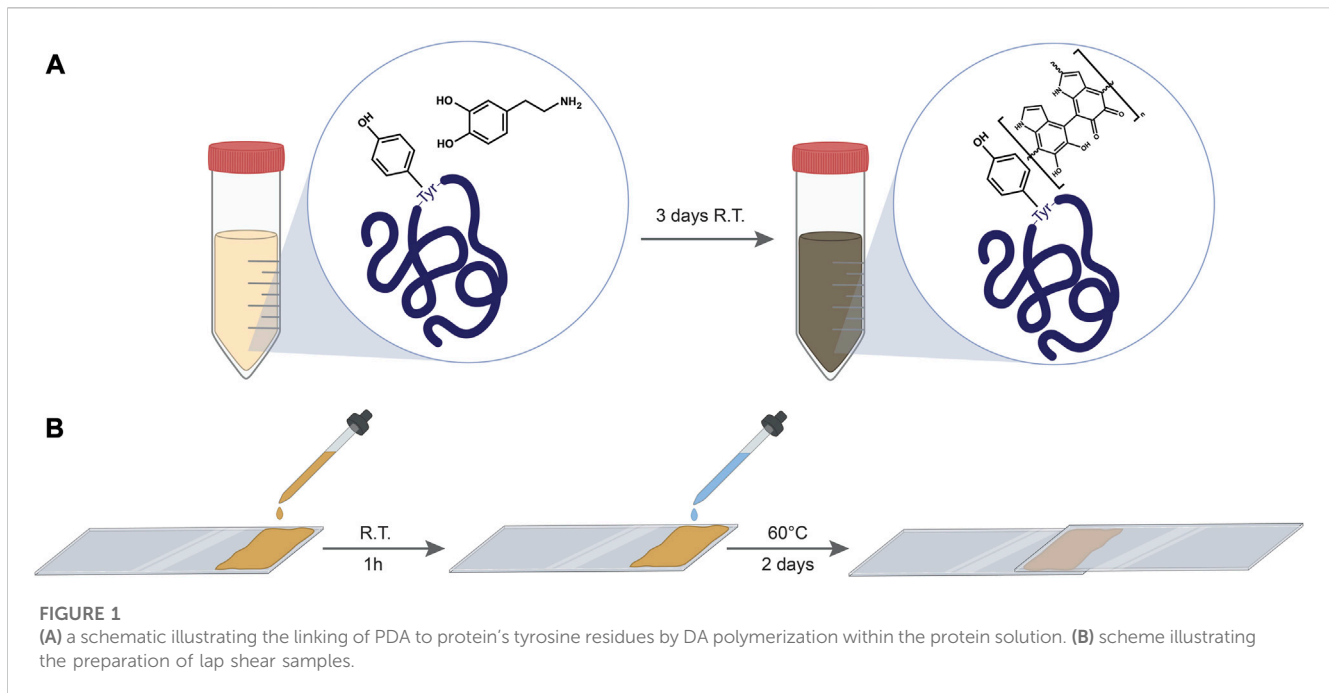
3 Results and discussion

Solutions of each protein (Casein, SF, SPH, BSA, OVA, WPI and Gelatin, 7% w/v) were mixed with DA solution with concentrations ranging from 20 to 360 mM, obtaining mixtures with DA:protein mass ratios from 1:20 to 1:1.

The solutions were left at room temperature for 3 days to allow spontaneous oxidative polymerization of DA and leading to the appearance of a brown color and the formation of bonds between PDA oligomers and proteins. Figure 1A schematized the bonding between PDA and tyrosine.

To test the bonding strength of the composites, protein-PDA solutions were cast on stainless-steel slides covering an area of $25 \times 7 \text{ mm}$. Figure 1B shows the general procedure employed to produce the testing specimens. After drying for 1 h, the films were activated with $10 \mu\text{L}$ of MilliQ water and a second slide was then placed atop the first one to create a lap shear joint. Subsequently, after 2 days at 60°C , a lap shear tensile strength test was performed, where the two adherents are pulled apart at a constant strain rate by a universal testing system, measuring the load vs. the extension (Supplementary Figures S1–S3) which can then be used to quantify the bonding strength of the adhesive.

Results reported in Figure 2 show the tensile strengths of the different adhesive compositions after the curing procedure. All the proteins-DA blends displayed a trend with a maximum bonding strength value corresponding to a different DA concentration (Figures 2A–G). To explain this trend, a comprehensive amino acid analysis was conducted for all the proteins used in our experiments (Supplementary Table S1), and we correlated the molar content of each amino acid with the molar content of dopamine in the blends that exhibited the highest bonding strength for each protein. Among all the amino acid to dopamine ratios examined, the ratio of tyrosine consistently displayed the most stable value for all the proteins used (Table 1). Our investigation revealed that in all instances, the highest bonding strength is achieved when DA is added at a molar excess to tyrosine of 8.6 ± 2.9 . (Figures 2A–G). Specifically, SF and casein (Figures 2A, B), which have a high tyrosine content (Supplementary Table S1) of 11.65% and 6.08% respectively, showed both maximum bonding strength with 220 mM of DA concentration. Conversely, SPH, BSA, OVA and WPI (Figures 2C–F) with a lower tyrosine content (Table 1) of 3.92, 4.83, 4.02, and 2.40% respectively, displayed their optimum bonding strength when 140 mM of DA was used with the same protein concentration (7%). Gelatin (Figure 2G), with the lowest tyrosine content of 0.88% displayed its maximum bonding strength at the



lowest DA concentration (40 mM). Among the various DA molar excess to tyrosine, the one that exhibits the greatest deviation is the excess associated with SF (4.4) (Table 1). This deviation can be attributed to the different availability of tyrosine residues in SF, as a substantial portion of tyrosines is buried within hydrophobic crystallites, making them inaccessible for the reaction (Freddi et al., 2006; Murphy and Kaplan, 2009). Previous studies investigating the chemical functionalization of tyrosine in SF have reported a reaction yield of 60% (Brown et al., 2017). Given a comparable yield in our process, the corresponding DA molar excess to tyrosine for silk fibroin would be 7.5.

Interestingly, in a report by Schmidt et al. (2018) regarding adhesives made using resorcinol and zein protein, optimal adhesive performance was found at a mass ratio at 16% and 84% respectively. In this study, the reported concentration of resorcinol is equivalent to 140 mM, matching the concentration where BSA, SPH, OVA and WPI demonstrated the most effective adhesion in our experiments (using DA). The observation that BSA, SPH, OVA and WPI possess a comparable amount of tyrosine content to zein (3.09%) (Yang et al., 2020) supports our findings. This also suggests that the optimal molar excess that we have reported works not only for dopamine, but also for other dihydroxy benzenes and it is therefore generalizable to other adhesives produced with protein and dihydroxy benzenes.

Figure 2H summarizes the best performance for all the proteins tested. It is worth noticing that the combination of readily available proteins and DA, water-curable adhesives with performances spanning from 0.6 MPa (OVA) to 10.9 MPa (gelatin) can be produced with this method. Performance over 1 MPa is often considered in the so-called “high-strength bonding range”.

To explain the observed optimal DA molar excess to tyrosine of 8.6 ± 2.9 , we propose that in this condition dopamine maximizes the size of pendant polydopamine (PDA) oligomers grafted onto the

protein chains, while minimizing the growth of unbound PDA polymers formed in solution. Our finding that bonding strength varies with the DA molar excess suggests that the major contribution to the binding of PDA to the protein chains occurs via the linkage of PDA to the tyrosine amino acid residue. This observation is further supported by the tendency of DA to preferentially form short oligomers (D’Ischia et al., 2014) of up to eight units. Therefore, a low DA concentration preferentially forms short PDA oligomers attached to proteins, while adding excess of DA results in the formation of free unlinked PDA oligomers as schematized in Figure 3. In the former case, the adhesive performance is suboptimal because the smaller pendant chains are less able to participate in cohesive interactions during curing process due to their short size and low number. In the case of an excess of DA, cohesion is lost due to DA-DA interactions happening between proteins and formation of unbound PDA oligomers, which fail to contribute to crosslinking interactions. At the optimal concentration the pendant PDA chains reach their terminal size (estimated at 8–11 DA subunits) but deplete the free DA and thus minimize formation of interfering unbound PDA oligomers.

As sketched in Figure 3, the 8.6 ± 2.9 DA molar excess to tyrosine likely leads to the best conditions for the formation of bound PDA oligomers that may cross-link different protein chains upon curing, leading to optimized performance when employed as adhesives. Similar results were previously reported in a study involving the binding of phenols to proteins (Mulaudzi et al., 2012) revealing that polyphenolic compounds display high protein affinity when they are small enough to penetrate inter-fibrillar regions of protein molecules but large enough to crosslink peptide chains at more than one point.

To further test our model, GPC was performed on SF solutions treated with different DA concentrations. GPC can detect changes in the molecular weight of SF and SF-PDA chains by measuring the elution time. The GPC technique also enables to estimate the degree

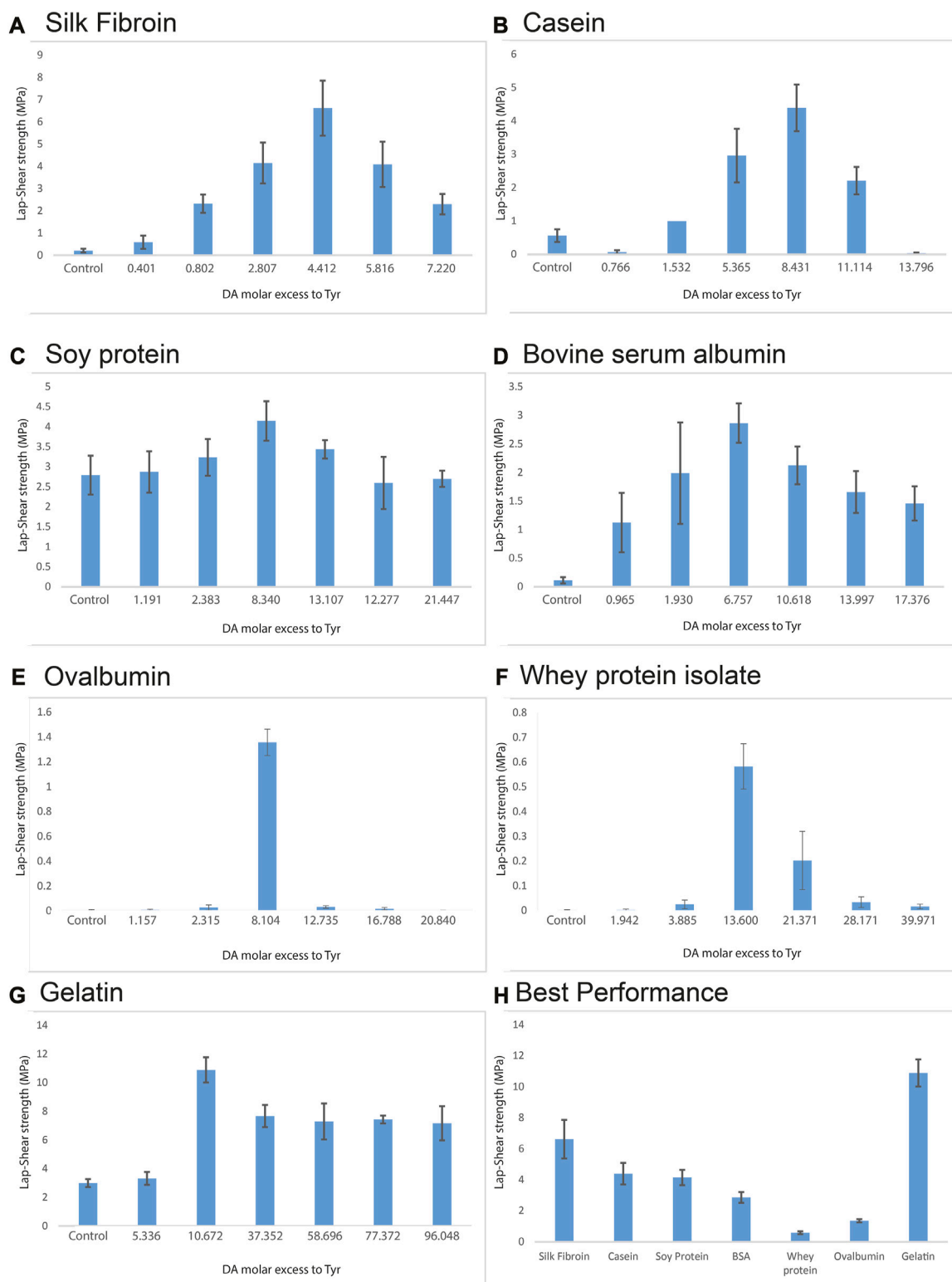


FIGURE 2

Lap shear strengths of adhesives blends made with (A) SF, (B) Casein, (C) Soy protein hydrolysate, (D) Bovine serum albumin, (E) Ovalbumin, (F) Whey protein isolate, (G) gelatin at different DA molar excess to tyrosine. (H) Best bonding strength performances for each protein. Error bars are the 95% confidence interval, $n = 5$ samples.

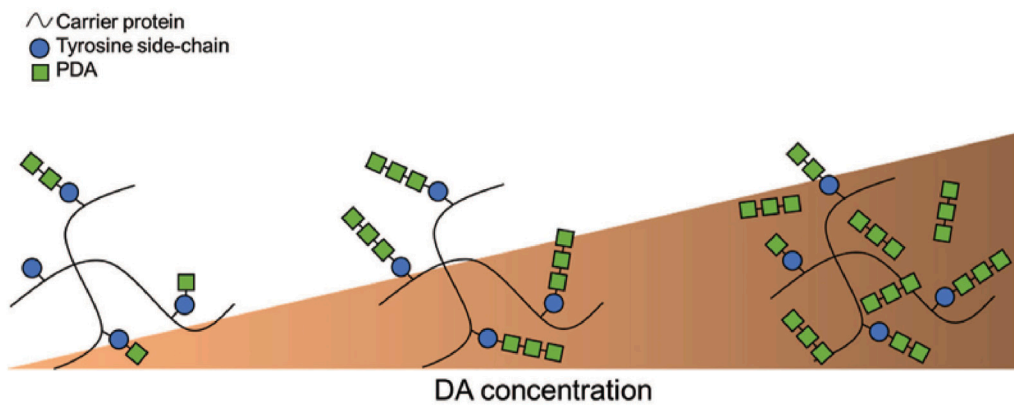


FIGURE 3
Schematic illustrating possible tyrosine's modification at increasing DA concentrations.

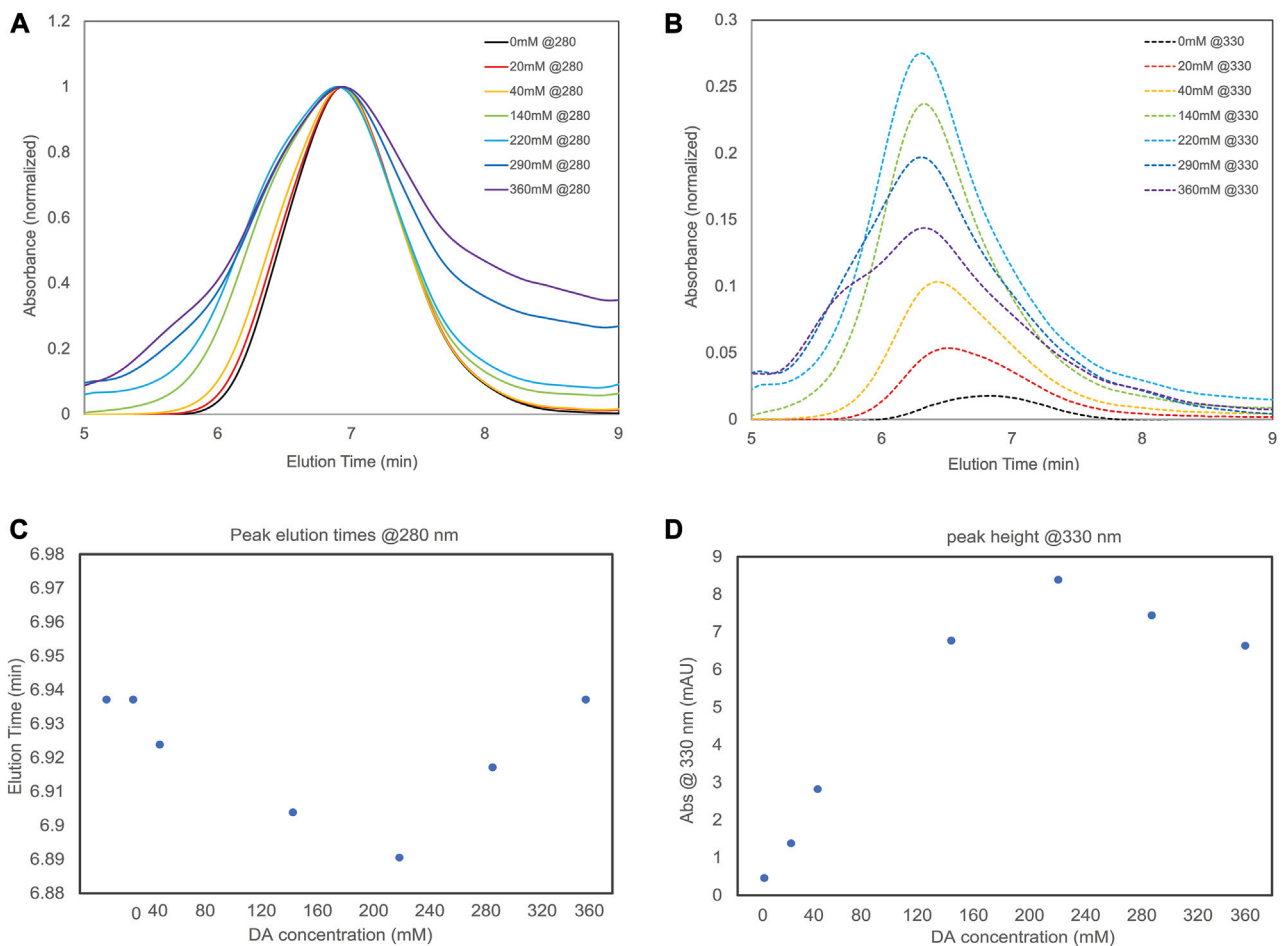
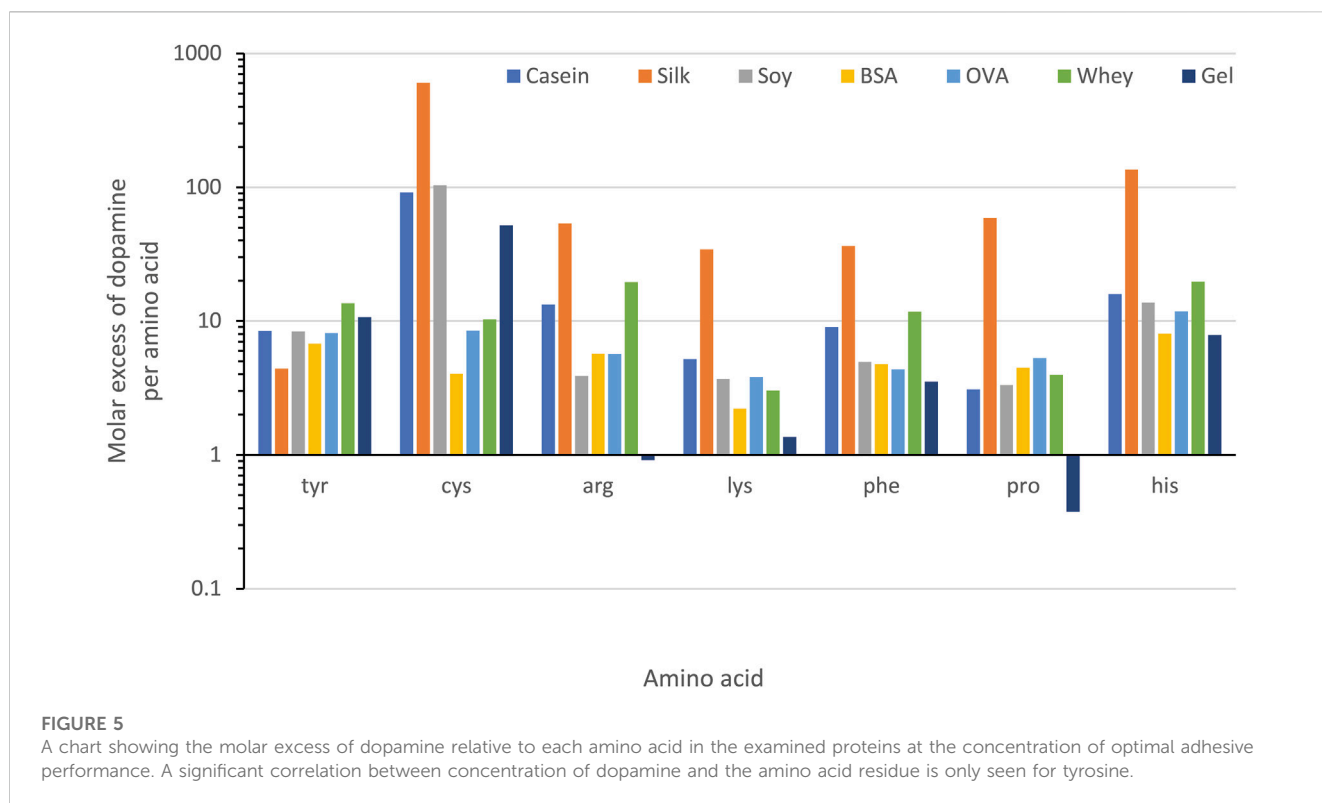


FIGURE 4
(A) A plot of absorbance at 280 nm vs. elution time of different SF-PDA blends (B) absorbance at 330 nm of the different SF-PDA blends. Both graphs are normalized to maximum absorbance at 280 nm (C) scatter plot reports the peak elution time of each blend observed at 280 nm (D) scatter plot reports maximum absorbance of each blend at 330 nm.



of SF functionalization with PDA by measuring the absorbance intensity (at 330 nm, [Supplementary Figure S5](#)).

[Figure 4A](#) and the related scatter plot in [Figure 4C](#) shows the elution times of SF treated with different DA concentrations. When DA is added at 220 mM, which is the concentration resulting in the highest adhesive performance and corresponds to a 4.4 DA molar excess to tyrosine, GPC shows the lowest peak elution time, indicating the greatest increase in molecular weight. Superior chain cross-linking from larger pendant oligomers during curing increases the cohesion of the material, explaining the increase in adhesive performance that occurred due to cohesive failures for all the specimens.

[Figure 4B](#) and the related scatter plot in [Figure 4D](#) shows the different elution's absorbance at 330 nm. This is directly correlated to the degree of DA functionalization on SF chains. Here again, when DA is at 220 mM (4.4 DA molar excess to tyrosine), the highest absorbance is detected, suggesting the highest degree of SF functionalization with PDA oligomers.

This supports our previous statement that when DA molar excess to tyrosine is 8.6 ± 2.9 , there is an increased DA-protein functionalization, while at higher DA concentration the formation of free PDA oligomers outcompetes the formation of pendant groups. Finally, to illustrate the correlation between optimal tyrosine and dopamine ratio, we calculated the molar excess of dopamine relative to other acid of interest ([Figure 5](#)) at the ratio of optimum bonding strength. For all the amino acids ([Supplementary Figure S6](#)) other than tyrosine, no correlation was found. Tyrosine is the sole amino acid showing consistent correlation with an excess of 0.13:1 Tyr:DA producing optimal adhesive properties for all the protein used ([Supplementary Table S2](#)).

4 Conclusions and outlook

In the search for a sustainable approach for manufacturing adhesives that makes exclusive use of renewable raw materials for a less petrochemically-reliant economy, we have presented a straightforward method for the creation of bioinspired adhesives using dopamine in combination with readily available proteins. We demonstrated a consistent correlation of adhesive performance with the rate of dopamine vs. tyrosine, which is absent for other amino acids. This study provides insight into a likely mechanism for adhesives based on curing-phase crosslinking between protein molecules by polydopamine oligomers as grafted onto tyrosine residues. As a consequence, we can calculate the value of excess DA vs. Tyr which optimizes bonding strength performances. We found that adding dopamine in 8.6 ± 2.9 excess with respect to the tyrosine content results in the highest adhesive performance across all proteins we have examined as well as other adhesives in the literature that function by exploiting protein/dihydroxy benzenes interactions.

As a final remark, the method does not involve the use of organic solvents or purification of reaction products. The obtained aqueous solutions can be cast and employed as adhesives requiring only water and heating for curing and still display increased adhesion performance from the pure protein from 1.5 (SPH) to 31.3 times (SF). In conclusion, we have reported a direct dependence on the bonding strength for adhesives made with protein and catechols thus providing insight into the fundamental mechanisms by which these adhesives work and how new adhesive systems may be optimized.

Data availability statement

The raw data supporting the conclusion of this article will be made available by the authors, without undue reservation.

Author contributions

All authors listed have made a substantial, direct, and intellectual contribution to the work and approved it for publication.

Funding

DB acknowledges funding from the REFIN (Return for Future Innovation) action, an initiative co-funded by the European Union through the POR Puglia 2014-2020 (Grant ID: 2455F798).

Acknowledgments

The authors thank the University of Michigan Proteomics and Peptide Synthesis Core for the amino acid analyses of the proteins used in this study.

References

- Ahn, B. K., Das, S., Linstadt, R., Kaufman, Y., Martinez-Rodriguez, N. R., Mirshafian, R., et al. (2015). High-performance mussel-inspired adhesives of reduced complexity. *Nat. Commun.* 6, 8663–8710. doi:10.1038/ncomms9663
- Arias, S., Amini, S., Krüger, J. M., Bangert, L. D., and Börner, H. G. (2021). Implementing Zn²⁺-ion and pH-value control into artificial mussel glue proteins by abstracting a His-rich domain from preCollagen. *Soft Matter* 17 (8), 2028–2033. doi:10.1039/d0sm02118k
- Bhagat, V., O'Brien, E., Zhou, J., and Becker, M. L. (2016). Caddisfly inspired phosphorylated poly(ester urea)-based degradable bone adhesives. *Biomacromolecules* 17 (9), 3016–3024. doi:10.1021/acs.biomac.6b00875
- Bilotto, P., Labate, C., De Santo, M. P., Deepankumar, K., Miserez, A., and Zappone, B. (2019). Adhesive properties of adsorbed layers of two recombinant mussel foot proteins with different levels of DOPA and tyrosine. *Langmuir* 35 (48), 15481–15490. doi:10.1021/acs.langmuir.9b01730
- Brown, J. E., Moreau, J. E., Berman, A. M., McSherry, H. J., Coburn, J. M., Schmidt, D. F., et al. (2017). Shape memory silk protein sponges for minimally invasive tissue regeneration. *Adv. Healthc. Mater* 6 (2), 1600762. doi:10.1002/adhm.201600762
- Burzio, L. A., and Waite, J. H. (2000). Cross-linking in adhesive quinoproteins: studies with model decapeptides. *Biochemistry* 39 (36), 11147–11153. doi:10.1021/bi0002434
- Chan Choi, Y., Choi, J. S., Jung, Y. J., and Cho, Y. W. (2014). Human gelatin tissue-adhesive hydrogels prepared by enzyme-mediated biosynthesis of DOPA and Fe³⁺ ion crosslinking. *J. Mater. Chem. B* 2 (2), 201–209. doi:10.1039/c3tb20696c
- Dalgaard, T. K., Nielsen, J. H., Brown, B. E., Stadler, N., and Davies, M. J. (2011). Dityrosine, 3,4-dihydroxyphenylalanine (DOPA), and radical formation from tyrosine residues on milk proteins with globular and flexible structures as a result of riboflavin-mediated photo-oxidation. *J. Agric. Food Chem.* 59 (14), 7939–7947. doi:10.1021/jf200277r
- Degtyar, E., Harrington, M. J., Politi, Y., and Fratzl, P. (2014). The mechanical role of metal ions in biogenic protein-based materials. *Angew. Chem. - Int. Ed.* 53 (45), 12026–12044. doi:10.1002/anie.201404272
- D'Ischia, M., Napolitano, A., Ball, V., Chen, C. T., and Buehler, M. J. (2014). Polydopamine and eumelanin: from structure-property relationships to a unified tailoring strategy. *Acc. Chem. Res.* 47 (12), 3541–3550. doi:10.1021/ar500273y
- Duconseille, A., Astruc, T., Quintana, N., Meersman, F., and Sante-Lhoutellier, V. (2015). Gelatin structure and composition linked to hard capsule dissolution: A review. *Food Hydrocoll.* 43, 360–376. doi:10.1016/j.foodhyd.2014.06.006
- Fratzl, P., and Barth, F. G. (2009). Biomaterial systems for mechanosensing and actuation. *Nature* 462 (7272), 442–448. doi:10.1038/nature08603
- Freddi, G., Anghileri, A., Sampaio, S., Buchert, J., Monti, P., and Taddei, P. (2006). Tyrosinase-catalyzed modification of *Bombyx mori* silk fibroin: grafting of chitosan under heterogeneous reaction conditions. *J. Biotechnol.* 125 (2), 281–294. doi:10.1016/j.jbiotec.2006.03.003
- Hofman, A. H., van Hees, I. A., Yang, J., and Kamperman, M. (2018). Bioinspired underwater adhesives by using the supramolecular toolbox. *Adv. Mater* 30 (19), 1704640. doi:10.1002/adma.201704640
- Horne, D. S. (2002). Casein structure, self-assembly and gelation. *Curr. Opin. Colloid Interface Sci.* 7 (5–6), 456–461. doi:10.1016/s1359-0294(02)00082-1
- Huang, W., Ling, S., Li, C., Omenetto, F. G., and Kaplan, D. L. (2018). Silkworm silk-based materials and devices generated using bio-nanotechnology. *Chem. Soc. Rev.* 47 (17), 6486–6504. doi:10.1039/c8cs00187a
- Jia, W., Jin, X., Liu, W., Zhao, B., Zhang, M., Yang, Y., et al. (2023). Evaluation the binding of chlorogenic acid with bovine serum albumin: spectroscopic methods, electrochemical and molecular docking. *Spectrochim. Acta - Part A Mol. Biomol. Spectrosc.* 291, 122289. doi:10.1016/j.saa.2022.122289
- Kaur, S., Weerasekare, G. M., and Stewart, R. J. (2011). Multiphase adhesive coacervates inspired by the sandcastle worm. *ACS Appl. Mater Interfaces* 3 (4), 941–944. doi:10.1021/am200082v
- Kohn, J. M., Riedel, J., Horsch, J., Stephanowitz, H., and Börner, H. G. (2020). Mussel-inspired polymerization of peptides: the chemical activation route as key to broaden the sequential space of artificial mussel-glue proteins. *Macromol. Rapid Commun.* 41 (1), 1900431. doi:10.1002/marc.201900431
- Kord Forooshani, P., and Lee, B. P. (2017). Recent approaches in designing bioadhesive materials inspired by mussel adhesive protein. *J. Polym. Sci. Part A Polym. Chem.* 55 (1), 9–33. doi:10.1002/pola.28368
- Krogsgaard, M., Nue, V., and Birkedal, H. (2016). Mussel-inspired materials: self-healing through coordination chemistry. *Chem. - A Eur. J.* 22 (3), 844–857. doi:10.1002/chem.201503380
- Krüger, J. M., and Börner, H. G. (2021). Accessing the next generation of synthetic mussel-glue polymers via mussel-inspired polymerization. *Angew. Chem. - Int. Ed.* 60 (12), 6408–6413. doi:10.1002/anie.202015833
- Lee, B. P., Messersmith, P. B., Israelachvili, J. N., and Waite, J. H. (2011). Mussel-inspired adhesives and coatings. *Annu. Rev. Mater. Res.* 41, 99–132. doi:10.1146/annurev-matsci-062910-100429
- Lo Presti, M., Giangregorio, M. M., Ragni, R., Giotta, L., Guascito, M. R., Comparelli, R., et al. (2020). Photoelectrodes with polydopamine thin films incorporating a bacterial photoenzyme. *Adv. Electron Mater* 6 (7), 2000140–2000211. doi:10.1002/aelm.202000140

Conflict of interest

The authors MLP, FO, and GF are also inventors of a patent (EP3986488A2) which partially describes the content of the manuscript.

The remaining authors declare that the research was conducted in the absence of any commercial or financial relationships that could be construed as a potential conflict of interest.

Publisher's note

All claims expressed in this article are solely those of the authors and do not necessarily represent those of their affiliated organizations, or those of the publisher, the editors and the reviewers. Any product that may be evaluated in this article, or claim that may be made by its manufacturer, is not guaranteed or endorsed by the publisher.

Supplementary material

The Supplementary Material for this article can be found online at: <https://www.frontiersin.org/articles/10.3389/fbiom.2023.1184088/full#supplementary-material>

- Lorenz, L. F., and Frihart, C. R. (2023). Ovalbumin has unusually good wood adhesive strength and water resistance. *J. Appl. Polym. Sci.* 140 (3). doi:10.1002/app.53332
- Lu, Q., Zhu, H., Zhang, C., Zhang, F., Zhang, B., and Kaplan, D. L. (2012). Silk self-assembly mechanisms and control from thermodynamics to kinetics. *Biomacromolecules* 13 (3), 826–832. doi:10.1021/bm201731e
- Ly, S., Dudek, D. M., Cao, Y., Balamurali, M. M., Gosline, J., and Li, H. (2010). Designed biomaterials to mimic the mechanical properties of muscles. *Nature* 465 (7294), 69–73. doi:10.1038/nature09024
- Mo, X., Zhong, Z., Wang, D., and Sun, X. (2006). Soybean glycinin subunits: characterization of physicochemical and adhesion properties. *J. Agric. Food Chem.* 54 (20), 7589–7593. doi:10.1021/jf060780g
- Muladziz, R. B., Ndhkala, A. R., Kulkarni, M. G., and Van Staden, J. (2012). Pharmacological properties and protein binding capacity of phenolic extracts of some Venda medicinal plants used against cough and fever. *J. Ethnopharmacol.* 143 (1), 185–193. doi:10.1016/j.jep.2012.06.022
- Murphy, A. R., and Kaplan, D. L. (2009). Biomedical applications of chemically-modified silk fibroin. *J. Mater. Chem.* 19 (36), 6443. doi:10.1039/b905802h
- Nam, S., Lee, S. Y., Kim, J. J., Kang, W. S., Yoon, I. S., and Cho, H. J. (2018). Polydopamine-coated nanocomposites of *Angelica gigas* Nakai extract and their therapeutic potential for triple-negative breast cancer cells. *Colloids Surfaces B Biointerfaces* 165, 74–82. doi:10.1016/j.colsurfb.2018.02.014
- Onwulata, C. I., and Tomasula, P. M. (2010). Gelling properties of tyrosinase-treated dairy proteins. *Food Bioprocess Technol.* 3 (4), 554–560. doi:10.1007/s11947-008-0124-4
- Ozdal, T., Capanoglu, E., and Altay, F. (2013). A review on protein-phenolic interactions and associated changes. *Food Res. Int.* 51 (2), 954–970. doi:10.1016/j.foodres.2013.02.009
- Peydayesh, M., Bagnani, M., Soon, W. L., and Mezzenga, R. (2023). Turning food protein waste into sustainable technologies. *Chem. Rev.* 123 (5), 2112–2154. doi:10.1021/acs.chemrev.2c00236
- Place, E. S., Evans, N. D., and Stevens, M. M. (2009). Complexity in biomaterials for tissue engineering. *Nat. Mater.* 8 (6), 457–470. doi:10.1038/nmat2441
- Presti, M. L., Rizzo, G., Farinola, G. M., and Omenetto, F. G. (2021). Bioinspired biomaterial composite for all-water-based high-performance adhesives. *Adv. Sci.* 2021, 2004786. doi:10.1002/advs.202004786
- Priemel, T., Degtyar, E., Dean, M. N., and Harrington, M. J. (2017). Rapid self-assembly of complex biomolecular architectures during mussel byssus biofabrication. *Nat. Commun.* 8, 14539. doi:10.1038/ncomms14539
- Rizzo, G., Lo Presti, M., Giannini, C., Sibillano, T., Milella, A., Matzeu, G., et al. (2020). Silk fibroin processing from CeCl₃ aqueous solution: fibers regeneration and doping with Ce(III). *Macromol. Chem. Phys.* 221 (13), 2000066–2000111. doi:10.1002/macp.202000066
- Rostamabadi, H., Chaudhary, V., Chhikara, N., Sharma, N., Nowacka, M., Demirken, I., et al. (2023). Ovalbumin, an outstanding food hydrocolloid: applications, technofunctional attributes, and nutritional facts, A systematic review. *Food Hydrocoll.* 139, 108514. doi:10.1016/j.foodhyd.2023.108514
- Saiz-Poseu, J., Mancebo-Aracil, J., Nador, F., Busqué, F., and Ruiz-Molina, D. (2019). The chemistry behind catechol-based adhesion. *Angew. Chem. - Int. Ed.* 58 (3), 696–714. doi:10.1002/anie.201801063
- Schmidt, G., Hamaker, B. R., and Wilker, J. J. (2018). High strength adhesives from catechol cross-linking of zein protein and plant phenolics. *Adv. Sustain. Syst.* 2 (3), 1700159–9. doi:10.1002/advs.201700159
- Shin, M., Shin, J. Y., Kim, K., Yang, B., Han, J. W., Kim, N. K., et al. (2020). The position of lysine controls the catechol-mediated surface adhesion and cohesion in underwater mussel adhesion. *J. Colloid Interface Sci.* 563, 168–176. doi:10.1016/j.jcis.2019.12.082
- Silverman, H. G., and Roberto, F. F. (2007). Understanding marine mussel adhesion. *Mar. Biotechnol.* 9 (6), 661–681. doi:10.1007/s10126-007-9053-x
- So, C. R., Scancelli, J. M., Fears, K. P., Essock-Burns, T., Haynes, S. E., Leary, D. H., et al. (2017). Oxidase activity of the barnacle adhesive interface involves peroxide-dependent catechol oxidase and lysyl oxidase enzymes. *ACS Appl. Mater. Interfaces* 9 (13), 11493–11505. doi:10.1021/acsami.7b01185
- Sui, X., Zhang, T., and Jiang, L. (2021). Soy protein: molecular structure revisited and recent advances in processing technologies. *Annu. Rev. Food Sci. Technol.* 12, 119–147. doi:10.1146/annurev-food-062220-104405
- Sun, J., Su, J., Ma, C., Göstl, R., Herrmann, A., Liu, K., et al. (2020). Fabrication and mechanical properties of engineered protein-based adhesives and fibers. *Adv. Mater.* 32 (6), 1906360–1906416. doi:10.1002/adma.201906360
- Topalá, T., Bodoki, A., Oprean, L., and Oprean, R. (2014). Bovine serum albumin interactions with metal complexes. *Clujul Med.* 87 (4), 215–219. doi:10.15386/cjmed-357
- Waite, J. H. (1990). The phylogeny and chemical diversity of quinone-tanned glues and varnishes. *Comp. Biochem. Physiol. - Part B Biochem.* 97 (1), 19–29. doi:10.1016/0305-0491(90)90172-p
- Wang, C. S., and Stewart, R. J. (2013). Multipart copolyelectrolyte adhesive of the sandcastle worm, *Phragmatopoma californica* (Fewkes): catechol oxidase catalyzed curing through peptidyl-DOPA. *Biomacromolecules* 14 (5), 1607–1617. doi:10.1021/bm400251k
- Wang, Y., Jeon, E. J., Lee, J., Hwang, H., Cho, S. W., and Lee, H. (2020). A phenol-amine superglue inspired by insect sclerotization process. *Adv. Mater.* 32 (43), 2002118–2002119. doi:10.1002/adma.202002118
- Webber, M. J., Appel, E. A., Meijer, E. W., and Langer, R. (2015). Supramolecular biomaterials. *Nat. Mater.* 15 (1), 13–26. doi:10.1038/nmat4474
- White, J. D., and Wilker, J. J. (2011). Underwater bonding with charged polymer mimics of Marine mussel adhesive proteins. *Macromolecules* 44 (13), 5085–5088. doi:10.1021/ma201044x
- Yang, J., Cohen Stuart, M. A., and Kamperman, M. (2014). Jack of all trades: versatile catechol crosslinking mechanisms. *Chem. Soc. Rev.* 43 (24), 8271–8298. doi:10.1039/c4cs00185k
- Yang, S., Zheng, M., Li, S., Xiao, Y., Zhou, Q., and Liu, J. (2020). Preparation of glycosylated hydrolysate by liquid fermentation with *Cordyceps militaris* and characterization of its functional properties. *Food Sci. Technol.* 40, 42–50. doi:10.1590/fst.37518
- Yuk, H., Wu, J., Sarrafian, T. L., Mao, X., Varela, C. E., Roche, E. T., et al. (2021). Rapid and coagulation-independent haemostatic sealing by a paste inspired by barnacle glue. *Nat. Biomed. Eng.* 5 (10), 1131–1142. doi:10.1038/s41551-021-00769-y
- Zeng, F., Wunderer, J., Salvenmoser, W., Ederth, T., and Rothbacher, U. (2019). Identifying adhesive components in a model tunicate. *Philos. Trans. R. Soc. B Biol. Sci.* 374, 20190197. doi:10.1098/rstb.2019.0197(1784)
- Zhan, K., Kim, C., Sung, K., Ejima, H., and Yoshie, N. (2017). Tunicate-inspired gallol polymers for underwater adhesive: A comparative study of catechol and gallol. *Biomacromolecules* 18 (9), 2959–2966. doi:10.1021/acs.biomac.7b00921
- Zhou, Z., Zhang, S., Cao, Y., Marelli, B., Xia, X., and Tao, T. H. (2018). Engineering the future of silk materials through advanced manufacturing. *Adv. Mater.* 30, 1706983. doi:10.1002/adma.201706983